OPTOELECTRONICS AND ADVANCED MATERIALS – RAPID COMMUNICATIONS Vol. 4, No. 8, August 2010, p. 1158 - 1162

The FTIR studies on the structural and electrical properties of SnO_2:F films as a function of hydrofluoric acid concentration

BO ZHANG[a,b], YUN TIAN[b], JIANXIN ZHANG[a,b], WEI CAI[a]
[a]*School of Materials Science and Engineering, Harbin Institute of Technology, Harbin, 150001. P. R. China*
[b]*School of Materials Science and Engineering, Shandong University, Jinan, 250061. P. R. China*

The fluorine doped tin oxide films were prepared using hydrofluoric acid as the fluorine precursor. The effect of hydrofluoric acid concentration on the film orientation, morphology and electrical parameters were discussed. The FTIR indicates that the fluorine ions prefer to substitute the oxygen ions in the group of O-Sn-O. While beyond a certain doping level, fluorine ions start to occupy interstitial sites, which has a negative effect on carrier concentration. The FTIR also shows the increase of the disorder of SnO_2 films with increasing fluorine doping. The main scattering centers of carriers are the impurity ions.

(Received July 20, 2010; accepted August 12, 2010)

Keywords: Tin oxide films, Spray pyrolysis, Substitution of fluorine for oxygen, Carrier

1. Introduction

Tin oxide (SnO_2) has been recognized as an attractive material with excellent optical properties, chemical durability and transparent conductivity [1]. Recent years have witnessed its extensive applications in solar energy, low-emission glass and heat mirrors [2,3]. However, the stoichiometric SnO_2 film has low electrical performance because of its low intrinsic carrier concentration. Doping with fluorine (F), antimony (Sb), chlorine (Cl), bromine (Br) and indium (In) has been achieved to improve its property [4-6]. Among these dopants, fluorine has been shown to be the most effective and achieved commercial use due to its low cost and simplicity.

Thin films of SnO_2 can be prepared by many techniques, such as chemical vapor deposition [7], sputtering [8], sol-gel [9], reactive evaporation [10], pulsed laser ablation [11], screen printing technique [12] and spray pyrolysis [13]. Among these techniques, spray pyrolysis is the most convenient method because it is simple, low cost, easy to add doping materials and promising for high rate and mass production capability of uniform large area coatings in industrial applications [13].

A survey of literature reveals that most research works focus on the fluorine doped SnO_2 films used ammonium fluoride (NH_4F) as a fluorine precursor. Recently, the use of SnF_2 has also been reported [14]. E. Elangovan et al. [15] have analyzed the reactions occurring in the deposition, they predicted the hydrofluoric acid (HF) is an intermediated production and the fluorine doping is achieved by the reaction between the SnO_2 and HF cloud around SnO_2 grains. The effective fluorine doping is possibly achieved by HF from decomposition of ammonium fluoride. However, the report of fluorine doped SnO_2 films with the HF as fluorine precursor is scarce. In this paper, we prepared the fluorine doped SnO_2 films with various HF concentrations in the deposition solution. The effects of HF concentration on the film structure, orientation and electrical parameters are investigated. The FTIR was used to estimate defects in the lattice, and the relationship between structure, FTIR and electrical parameters is also discussed.

2. Material and methods

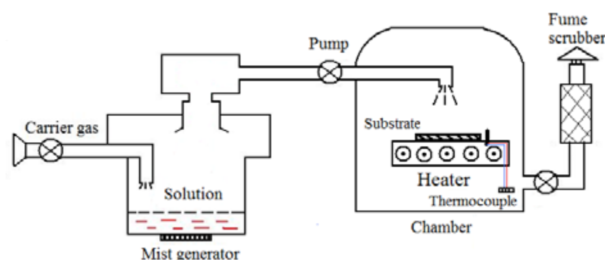

Fig. 1. The setup of Ultrasonic Spray Pyrolysis equipment.

An aqueous solution of high pure tin chloride ($SnCl_2 \cdot 2H_2O$) was used as starting solution for deposition. The concentration of the solution was 0.1mol/L. A small amount of concentrated hydrochloric acid (HCl) was added to the undoped solution to prevent hydrolysis. Fluorine doping was achieved by adding hydrofluoric acid (HF) to the solution. The ratio of the molar concentration between fluorine and tin fixed at 0, 0.25, 0.50, 0.75, 1.0 and 1.25.

The SnO_2 films were prepared by an ultrasonic spray pyrolysis coating setup as Fig. 1. The films were grown on the soda-lime glass substrates and KBr for FTIR. The deposition temperature was 350 ^oC, which is as low as possible to obtain the crystal film. The atomization rate was 1~3 ml/min, and compressed air was used as carried gas. The spray process was not continuous with an

intermittence to keep the temperature of substrates. The samples were naturally cooled down after deposition.

The crystalline characteristic of SnO_2 films was studied by XRD (RINT-2200, Rigaku) using Cu *K*α radiation. The FTIR measurement was conducted in transmission model using a Fourier transform spectrophotomerer (Victor 22, Bruker). The morphology was obtained by Scanning Electron Microscope (SEM) (JSM6610lv, JEOL). The carrier concentration and mobility were carried out by Hall measurement (Ecopia, HMS3000) in van der Pauw configuration at room temperature.

3. Results and discussion

3.1 Structural studies

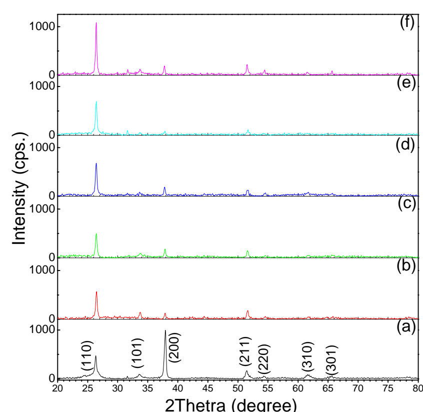

Fig. 2. The X-Ray diffraction patterns of fluorine doped SnO_2 films: (a) F/Sn 0at.; (b) F/Sn 0.25at. ; (c) F/Sn 0.50at.; (d) F/Sn 0.75at.; (e) F/Sn 1.0at.; (f)F/Sn1.25at.

The X-ray diffraction patterns of SnO_2 films with various HF concentrations are shown in Fig. 2. All the films are found to be of cassiterite type with a tetragonal rutile structure. The undoped SnO_2 film displays a preferred orientation of (200) whereas all fluorine doped SnO_2 films grow along (110) irrespective of doping level. Presence of weak reflections such as (101), (211), (220), (310) and (301) have also been detected with lower intensities. There is no feature of fluoride and chloride observed in the patterns, suggesting the complete incorporation of fluorine and the oxidation of stannous.

Kojima et al. [16] have reported that the SnO_2 films prepared at 350 ^{o}C are amorphous. The possible reason can be sought from the decomposition of solutions. Since the crystallization of the films in the spray method depends on the proper decomposition, their high molar concentration in their study may result in an improper decomposition at this low temperature. This is confirmed by their report [17], in which their films were consequently crystallized when the concentration of solution was decreased or at high deposition temperature.

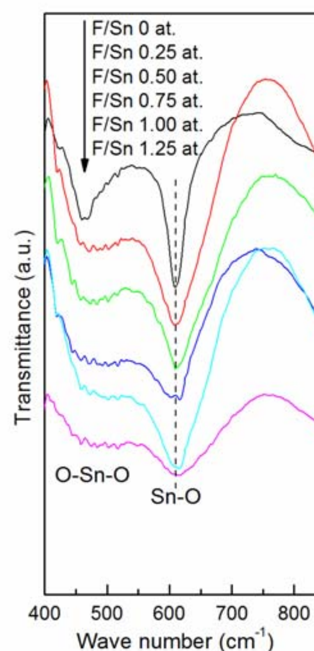

Fig. 3. The FTIR spectrums of fluorine doped SnO_2 films.

The characteristic of preferred orientation in SnO_2 films has been shown to depend on the preparation. D. J. Goyal et al. [18] have reported at low doping concentration, the SnO_2 film growth is along (110), and it changes gradually to (200) with an increase in concentration. It also has reported that the SnO_2 films have a disordered growth for stannous precursor. But in the present case, the preferred orientation of (110) for fluorine doped SnO_2 films remains predominant for all doping levels. This consistency in orientation suggests that the precursor solution has uniformity in the composition. The introduction of fluorine is a reason for the growth along (110). The various orientation between the undoped and fluorine doped SnO_2 films can be ascribed to the additives in solution, which are HCl and HF for the undoped and doped solution respectively. The additive HCl makes the film has a tendency of orientation along (200) due to the formation of intermediate molecules. When HCl is added to $SnCl_2$ solution, HCl will associate with tin dichloride to give a neutral $HSnCl_3$ molecule. $HSnCl_3$ is known to be unstable and very reactive. Once in the pyrolysis region, it is oxidized by H_2O and gives a hydrated SnO_2 molecule which can react quickly to form SnO_2 films along (200) as bulk material. Smith et al. [19] also observed the (200) preferred orientation for SnO_2 films deposited from $SnCl_2$ and HCl by spray pyrolysis.

The FTIR spectrum is employed to examine the details in the structure. Selected region of the recorded spectrum for SnO_2 films are shown in Fig. 3. The main IR features of SnO_2 appear at 461 and 609 cm^{-1}, which assign to O-Sn-O and Sn-O stretching vibration respectively [20]. The feature of O-Sn-O is broadening and weakening

gradually as the fluorine doping increases. An obvious shift of Sn-O vibration frequency from 609 cm^{-1} to 617cm^{-1} is found once the doping level exceeds F/Sn 0.50at.

The broadening of O-Sn-O feature can ascribe to the substitution in the film. In the fluorine doped SnO_2 films, the fluorine ions(F^-) have been supposed to substitute oxygen ions (O^{2-}) as following reasons[21]: their similar ionic size(F^-~ 0.133 nm, O^{2-}~ 0.132 nm), the comparable bond energy with Sn(Sn-O bond ~ 31.05 D°/kJ mol^{-1}, Sn-F bond~26.75 D°/kJ mol^{-1}), and Coulomb forces that bind the lattice together are reduced, since the charge on the F^- is only half of the charge of the O^{2-}. Thus, geometrically the lattice is nearly unable to distinguish between F^- and O^{2-}. The substitution of fluorine for oxygen destroys the vibration model of O-Sn-O group and it also can increase the defect in SnO_2 lattice because of lattice mismatch. So the O-Sn-O feature displays a broadening and weakening process. The long bond length (O-Sn-O:2.597 Å; Sn-O:2.053 Å) can account for occurring of substitution on O-Sn-O group. However, there is a solubility limit of fluorine atoms in SnO_2 lattice beyond which the excess fluorine atoms could not replace the oxygen in the lattice, but form the interstitial fluorine. The presence of interstitial fluorine increases the disorder of lattice markedly, which causes the shift of Sn-O vibration frequency after doping of F/Sn 0.75 at. Therefore, all the incorporation process of fluorine atoms in SnO_2 lattice is well indicated by the FTIR, especially the solution limit of fluorine.

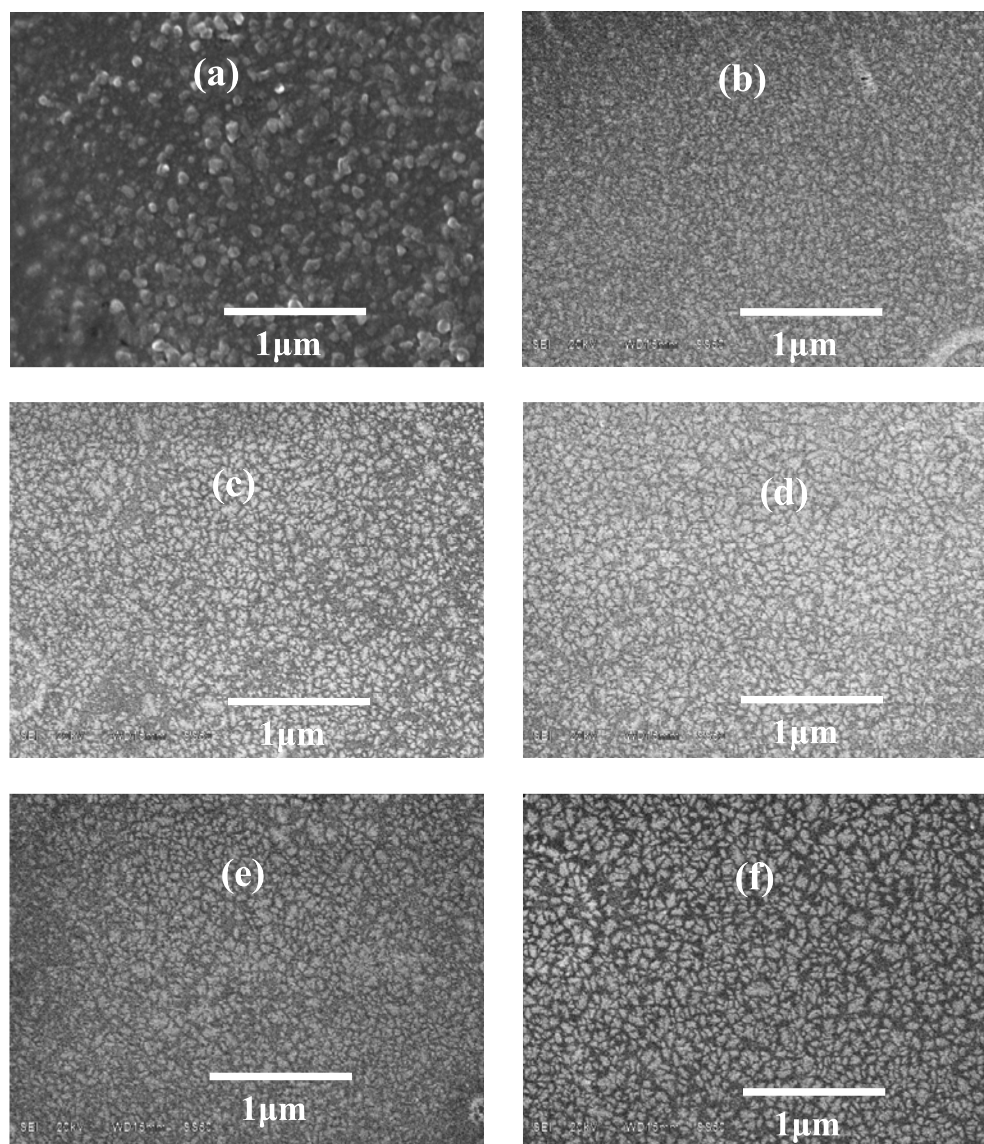

Fig. 4. The morphology of fluorine doped SnO_2 films: (a) F/SnCl 0at.; (b) F/Sn 0.25at. ; (c) F/Sn 0.50at. ; (d) F/Sn 0.75at. ; (e) F/Sn 1.0at.; (f) F/Sn 1.25at.

3.2 Morphological studies

The SEM images recorded on the surface of the SnO_2 films are shown in Fig. 4. The surfaces are found to be uniform and homogeneous. The undoped SnO_2 film shows strip shaped particles on the surface, while corrugated morphologies cover the surfaces of fluorine doped SnO_2 films. These various morphologies can ascribe to the different preferred orientation along (200) and (110) in the growth. E. Elangovan et al. [22] have reported the similar shaped particles with preferred orientation along (200). Smith et al. [19] have done the morphological simulation of SnO_2 crystals, and their results further confirmed these strip shaped particles was a result of growth along (200). The corrugated morphology has not been reported in the literatures. The corrosion reaction between HF and substrate may be the reason for the fluctuant surface.

3.3 Electrical studies

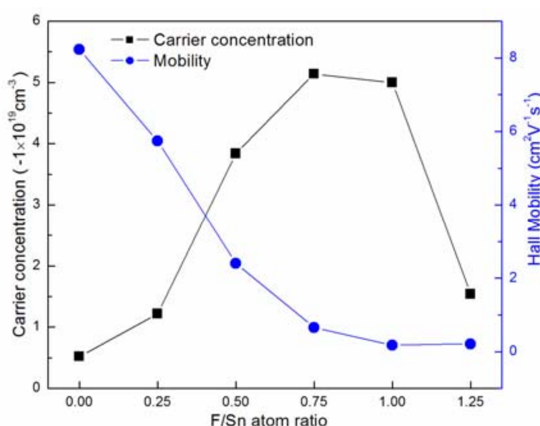

Fig. 5. The carrier concentration and Hall mobility of fluorine doped SnO_2 films.

The various carrier concentration and Hall mobility as a function of fluorine doping level are described as Fig. 5. The carrier concentration shows an increase till F/Sn 0.75at., and then decreases as the doping concentration increases. As the n-type semiconductor, their free electrons of SnO_2 films come from the substitution of dopant serving as donors. In the fluorine doped SnO_2 films, each F^- substitutes an O^{2-} in the lattice and the substituted O^{2-} provides one free electron [22]. More F^- substitute the O^{2-} in the lattice and more free electrons are produced that, in turn, results in an increase of carrier. But when the fluorine concentration is more than the solution limit of fluorine in the lattice, the excess fluorine atoms would form interstitial fluorine. The interstitial fluorine cannot provide free electrons, but capture the free electrons, which causes a decrease of carrier is displayed once the doping level exceeds the doping of F/Sn 0.75at. This process of fluorine incorporation is in good agreement with the results from the FTIR.

The mobility of SnO_2 films shows a continuous decrease from 8.2 $cm^2V^{-1}s^{-1}$ to 0.6 $cm^2V^{-1}s^{-1}$ as the fluorine doping level increases. The actual value of mobility is determined by the interaction between the various scattering centers and free carriers. In the films prepared by spray pyrolysis method, an ideal lattice cannot be expected, even if no donor atoms are present. Hence, the scattering of electrons by the thermal vibration of the lattice atoms can omitted in the case [23]. It have verified grain boundary and impurity ion scattering are the possible dominant scattering mechanism in the films. The condition of grain boundary scattering to be dominant is the mean free path values should be comparable to crystallite size [24]. In the present case, we calculate the mean free path according to the degeneracy model and find the mean free path does not exceed 5nm, which is considerable shorter than grain size. Thus, scattering due to grain boundary is not the main scattering. Recently, Gilmore et al.[25] have reported that the influence of grain boundary is in a different manner and they though the optical mobility is not impacted by grain boundary as long as the grain size is much greater than the mean free path. The impurity ions should be the scattering centers of the carriers, which leads to the decrease of mobility.

4. Conclusion

The fluorine doped SnO_2 films were prepared using the hydrofluoric acid as the fluorine precursor. The films show a preferred orientation along (110) and corrugated morphology irrespective of doping levels. The incorporated fluorine ions would substitute the oxygen ions to provide free electrons and then occupy the interstitial site. This rule of fluorine atoms is well reflected by the FTIR and carrier concentration. The feature of Sn-O in FTIR indicates the solution limit of fluorine in SnO_2 lattice. The impurity ions scattering is the main scattering mechanism occurring in the films.

Acknowledgement

The authors gratefully thank Doctor Lili Wu and Yongxin Qi (Shandong University) for assistance in characterization.

References

[1] E. Fortunato, D. Ginely, H. Hosono, D. C. Paine, MRS Bull. **32**, 242-247 (2007).
[2] A. V. Moholkar, S. M. Pawar, K. Y. Rajpure, C. H. Bhosale, J. H. Kim, Applied Surface Science **23**, 9358-9364 (2009).
[3] E. Kuantama, D. W. Han, Y. M. Sung, J. E. Song, C. H. Han, Thin Solid Films. Thin Solid Films **517**, 4211-4214 (2009).
[4] S. K. Ghandhi, R. Siviy, J. M. Borrego, Appl. Phys.

Lett. **34**, 833-836 (1979).
[5] C. Schaefer, G. Brauer, J. Szczyrbowski, Surface and Coatings Technology. **93**, 37-45(1997).
[6] C. G. Fonstad, R. H. Rediker, Journal of Applied Physics. **42**, 2911(1971).
[7] J. R. Brown, P. W. Haycock, L. M. Smith, A. C. Jones, E. W. Williams. Sensor Actuators B **63**,109-114 (2000).
[8] S. Boycheva, A. K. Sytchkova, M. L. Grilli, A. Piegari, Thin Solid Films **515**, 8469-8473 (2007).
[9] A. N. Banerjee, S. Kundoo, P. Saha, K. K. Chattopadhyay. Journal of Sol-gel Science and Technology **28**, 105 (2003).
[10] K. Omura, P. Velucham, M. Tsuji, T. Nihio, M. Murozono. Journal of Electrochemistry Society. **146**, 2113-2116 (1999).
[11] J. H. Kim, K. A. Jeon, G. H. Kim, S. Y. Lee. Applied Surface Science. **252**, 4834-4837 (2006).
[12] J. J. Berry, D. S. Ginley, P. E. Burrows, Applied Physics Letter. **92**, 193304-193307 (2008).
[13] M. Ruske, G. Brauer, J. Szczyrbowski, Thin Solid Films **351**, 146-150 (1999).
[14] G. C. Morris, A. E. McElnea, Applied Surface Science **92**, 167 ~199 (1996).
[15] E. Elangovan, M. P. Singh, K. Ramamurthi, Materials Science and Engineering B **113**, 143-148 (2004).
[16] M. Kojima, H. Kato, M. Gatto, Philos. Mag. B **73**, 277 (1996).
[17] M. Kojima, H. Kato, Philos. Mag. B **73**, 289 (1996).
[18] D. J. Goyal, Chitra Agashe, B. R. Marathe, M. G. Takwale, V. G. Bhide. J. Appl. Phys. **73**, 7520-7523 (2002).
[19] A. Smith, J. M. Laurent, D. S. Smith, J. P. Bonnet, R. R. Clemente, Thin Solid Films **266** ,20-30 (1995).
[20] Endrowednes Kuantama, Deok-Woo Han, Youl-Moon Sung, Jae-Eun Song, Chi-hwan Han, Thin Solid Films. **517**, 4211-4214 (2009).
[21] E. Elangovan, K. Ramamurthi, Applied Surface Science **249**, 183–196 (2005).
[22] E. Elangovan, K. Ramesh, K. Ramamurthi, Solid State Communications **130**, 523-527 (2004).
[23] J. J. Ph. Elich, E. C. Boslooper, H. Haitjema, Thin Solid Films **177**, 17-33 (1989).
[24] B. Thangaraju, Thin Solid Films **402**, 71-78 (2002).
[25] A. S. Gilmore, A. Al-Kaoud, V. Kaydanov, T. R. Ohno, Mate. Res. Soc. Symp. Proc. **666**, F3.10.1 (2001).

*Corresponding author: zhangbo8803@163.com